Novel Toll-like Receptor 2 Ligands for Targeted Pancreatic Cancer Imaging and Immunotherapy

Amanda Shanks Huynh[1], **Woo Jin Chung**[2], **Hyun-Il Cho**[3], **Valerie E. Moberg**[1], **Esteban Celis**[3], **David L. Morse**[1,*], and **Josef Vagner**[2,*]

[1]Dept. Cancer Imaging & Metabolism, H. Lee Moffitt Cancer Center & Research Institute, 12902 Magnolia Drive, Tampa, FL 33612, United States.

[2]The BIO5 Research Institute, University of Arizona, 1657 E Helen Street, Tucson, Arizona 85721, United States.

[3]Dept. Immunology, H. Lee Moffitt Cancer Center & Research Institute, Tampa, FL; USA

Abstract

Toll-like receptor 2 (TLR2) is a target for immune system stimulation during cancer immunotherapy and a cell-surface marker for pancreatic cancer. To develop targeted agents for cancer imaging and therapy, we designed, synthesized and characterized thirteen novel, fully synthetic high affinity TLR2 agonists. Analog **10** had the highest agonist activity (NF-κB functional assay, EC_{50}=20 nM) and binding affinity (competitive binding assay, K_i=25 nM). As an immune adjuvant, compound **10** stimulated the immune system *in vivo* by generation and persistence of antigen-specific CD8+ T cells indicating its potential use in cancer immunotherapy. After conjugation of near-infrared dye to **10**, agonist activity (EC_{50}=34 nM) and binding affinity (K_i =11 nM) were retained in **13**. Fluorescence signal was present in TLR2 expressing pancreatic tumor xenografts 24 h post-injection of **13**; while an excess of unlabeled ligand blocked **13** from binding to the tumor resulting in significantly decreased signal (p<0.001) demonstrating *in vivo* selectivity.

Keywords

Toll-like Receptor 2; Solid-phase Synthesis; Functional Bioassays; Binding Assays; Time-resolved Fluorescence; Peptidomimetic; Targeted Fluorescence Imaging; Immunotherapy; Pancreatic Cancer; TLR2 Agonist Ligands

INTRODUCTION

The discovery of ligands and small-molecular-mass synthetic compounds that specifically activate Toll-like receptor 2 (TLR2) has raised interest in this cell-surface receptor as a potential target for the development of new therapies, including the treatment of cancer.[1]

*Corresponding Authors phone, 520-626-4179; fax, 520-626-4824; vagner@email.arizona.edu. . *phone, 813-745-8948; fax, 813-745-8357; david.morse@moffitt.org. .

TLR2 has a role in activation and regulation of the innate immune system and targeted stimulation of this receptor has been used to augment cancer immunotherapy.[1b, 2] Although TLR2 is predominantly expressed in tissues involved in immune function, the expression profile varies among tissues and cell types.[3] TLR2 is a type I transmembrane glycoprotein characterized by an external antigen recognition domain comprised of a highly conserved leucine-rich repeat motif, a transmembrane domain, and a cytoplasmic Toll/interleukin-1 (TIR) receptor homology signaling domain. Intracellular signaling is activated by agonist binding and is facilitated by the formation of the cytoplasmic TIR domain through heterodimerization with either TLR1 or TLR6.[4] TLR2 is a pattern recognition receptor with the ability to recognize pathogen-associated molecular patterns (PAMPs).[5] Stimulation by PAMPs initiates signaling cascades that activate NF-κB transcription factors inducing the secretion of pro-inflammatory cytokines and effector cytokines directing the immune response.[5c]

The potential use of synthetic TLR2 agonists for the enhancement of cancer immunotherapy is an active area of research.[6] There are four mechanisms by which TLR2 stimulation may produce significant antitumor activity: enhancement of the innate immunity, enhancement of T-cell immunity, enhancement of cytotoxic antibody function, and induction of apoptosis in TLR2-positive tumors.[1b] Examples include, the TLR2 induction of tumor necrosis factor-α (TNF-α), increasing the production of nitric oxide synthase (iNOS) and thus inducing apoptosis of chemotherapy-resistant tumor cells,[7] reduction of bladder tumor growth by TLR2 agonist, SMP-105;[8] and a combination therapy of macrophage-activating lipopeptide 2-kDa (MALP-2) and gemcitabine increased the survival rates of incompletely resectable pancreatic cancers in a phase l/ll trial.[9] We have previously reported the use of TLR agonists as immune adjuvants that can increase the magnitude and duration of peptide vaccine-induced T cell responses;[10] as demonstrated by our TriVax vaccine that elicits potent protective antitumor immunity as well as remarkable therapeutic effects against melanoma.[11]

In an effort to improve the less than 6% 5 year survival rate for pancreatic cancer,[12] we are investigating the potential of TLR2 ligands for use in targeted pancreatic cancer imaging and treatment. Improved survival rates are associated with the surgical resection of the primary tumor if the tumor tissue is completely removed at the margins.[13] However, it is a high risk procedure with a low success rate due to difficulty in clearly identifying tumor tissue from normal tissue, resulting in positive resection margins (R_1).[14] The development of new intraoperative surgical methods employing fluorescence guided tumor detection could lead to increased negative resection margins (R_0) resulting in improved survival rates. Recent clinical studies involving image-guided surgeries have demonstrated the potential of this approach.[15] We have previously reported TLR2 as a bona fide cell surface marker for pancreatic cancer that is highly expressed in 70% of pancreatic tumors but is not highly expressed in surrounding normal pancreas tissue.[16] Fluorescence imaging probes developed using TLR2 specific ligands could be applied to the intraoperative detection of pancreatic tumor margins.

A variety of microbial component derived lipopeptides (LPs) are recognized as TLR2 ligands. For example, mycoplasma produce diacylated MALP-2, Cys(*S*-[2,3-bisacyloxy-(R)-propyl])-Gly-Asn-Asn-Asp-Glu-Ser-Asn-Ile-Ser-Phe-Lys-Glu-Lys, binds to the TLR2/TLR6 heterodimer.[17] The structure-activity relationships (SAR) of TLR2 binding and stimulation of the immune system for many synthetic LPs are well documented in the literature. Both the well-characterized synthetic di- and tri-acylated LP ligands, Pam_2CSK_4 and Pam_3CSK_4, bind to internal protein pockets through hydrophilic interactions to selectively induce signaling via the TLR2/TLR6 and TLR2/TLR1 heterodimers, respectively.[4b, 17c, 18] In addition to LPs, the serum amyloid A protein (SAA) was recently

identified as a potent TLR2 agonist by Cheng *et al*., and is a major acute-phase protein that is considered to be a marker for inflammatory diseases.[1a, 19]

TLR2 specific agonist ligands developed herein have potential for use in both the development of targeted agents for the imaging and treatment of pancreatic cancer, and as an adjuvant for cancer immunotherapy. In an effort to identify novel TLR2 ligands that are highly potent TLR2 agonists for use in immunotherapy, or ligands with high binding affinity for TLR2 with potential for attachment of imaging contrast and therapeutic agents, we have iteratively synthesized two sets of rationally designed synthetic compounds and investigated their SAR by *in vitro* functional bioassays, *in cyto* binding assays, *in vivo* immune system stimulation and molecular imaging studies demonstrating tumor specificity. From the crystal structure of TLR2 complexes, it is known that the minimal ligand recognition structure contains a Cys(*S*-[2,3-bis(palmitoyl)oxy-(R)-propyl] residue.[18d] Therefore, we kept this pharmacophore element and made changes to the flexible peptide component. The rationale behind this design strategy was to remove the metabolically unstable peptide and the positively charged tetralysine moiety, and substitute them with indifferent and hydrophobic polyethylene glycol chains. The goal of this design strategy was to discover water soluble ligands without compromising potency and this was achieved for compounds **10**, **11** and **13** (*vide infra*). Compound **10** has potent bioactivity (20 nM EC_{50}), high affinity binding (24 nM K_i) and effective immune system stimulation. After conjugation of a near-infrared fluorescent dye to **10** generating **13**, high bioactivity (34 nM EC_{50}) and binding affinity (11 nM K_i) were retained, and tumor specificity was observed *in vivo* by fluorescence imaging of mice bearing TLR2 expressing tumor xenografts. In addition, **10** has a greatly simplified synthesis strategy with improved solubility and a built-in attachment point for imaging contrast and/or a therapeutic moiety.

RESULTS

TLR2 Ligand Library Design and Synthesis

Thirteen novel fully synthetic compounds were designed and synthesized to discover novel TLR2 specific ligands with the desired properties of high specificity, high agonist activity, high binding affinity, solubility and built-in attachment points for conjugation of fluorescent dyes and chelates. Initially, seven compounds (**1-7**) based on the structure of the bispalmitoylated MALP-2,[17a] Cys(*S*-[2,3-bis(palmitoyl)oxy-(R)-propyl])-Gly-Asn-Asn-Asp-Glu-Ser-Asn-Ile-Ser-Phe-Lys-Glu-Lys, were synthesized. Each compound in the set was comprised of the same scaffold, X-Cys(*S*-[2,3-bis(palmitoyl)oxy-(R)-propyl])-Gly-Asn-Asn-Asp-Glu-Ser-Asn-Ile-Ser-Phe-Lys-Glu-Lys-NH_2, or X-MALP-2 where the X-group represents an N-terminal modification (Table 1, Supporting Information Figure 5).

After screening compounds **1-7** for bioactivity (*vide infra*), a second set of three compound analogs (**8-10**) was designed based on SAR knowledge gained from the first set. The scaffold, Ac-PEGO-Cys(*S*-[2,3-bis(palmitoyl)oxy-(R)-propyl])-Y, was derived using compound **3**'s N-terminal modification of the MALP-2 LP that included an acetylated 20 atom ethylene glycol oligomer(PEGO) plus Y modifications at the C-terminus (Table 1). Compound **8**'s Y-group modification was derived from a CD14 peptide known to induce the physical proximity of CD14, TLR2 and TLR1.[20] Compound **9**'s Y-group modification was derived from a *S. aureus* peptide that should be more acidic or at least neutral compared to the recently identified potent TLR2 agonist, serum amyloid A (SAA) by Cheng *et al*.[1a, 21] To test the importance of the peptide component of MALP-2 in terms of potency, compound **10**'s Y-group modification was derived from compound **3**'s structure with the peptide component reduced to a short Gly-DSer linker with a PEGO-NH_2 at the C-terminus to enhance solubility.

Since compound **10** was determined to have the most potent TLR2 bioactivity (*vide infra*), three final compounds were designed and synthesized to incorporate at the N-terminus, in lieu of the acetyl group, a europium diethylenetriaminepentaacetic acid (Eu-DTPA) chelate (compound **11**), 3-mercaptopropionyl residue (Mpr) for attachment to thiol groups (compound **12**), and the near-infrared dye IRDye800CW (LI-COR, Lincoln, NE, USA) functionalized with Mpr for attachment (compound **13**) (Scheme 1, Table 1). Compound **11** was used to determine TLR2 binding affinity via *in cyto* time-resolved fluorescence (TRF) binding assays. Compound **13** was used for *in vivo* fluorescence imaging to determine TLR2 specificity and binding.

In Vitro Functional Bioassay

We developed a functional bioactivity assay to specifically detect intracellular signaling induced by agonist stimulation of the human TLR2 receptor at the cell-surface. This assay underwent optimization prior to starting our peptide screenings. Optimal NF-κB induced expression of luciferase led to observed luminescence 48 h post transient transfection and 24 h post ligand stimulation. Luminescence intensity was significantly greater (50-fold, n = 6, p<0.001) in Pam_3CSK_4 and stimulated HEK-293/hTLR2 cells relative to cells incubated with no ligand (Supporting Information Figure 1C). The ligand-stimulated parental HEK-293 cells had no measurable luminescence. Hence, the measured luminescence is specifically induced by signaling of TLR2 agonists via the NF-κB pathway.

We initially screened the first set of seven MALP-2 derived compounds (**1**-**7**) with N-terminal modifications (Table 1) to determine *in vitro* TLR2 agonist activity. All seven of the compounds exhibited comparable levels of NF-κB induced luminescence relative to the reference TLR2 agonist ligand controls (Figure 1A). The control, Pam_2CSK_4, is a synthetic diacylated lipopeptide with the same palmitic acid pharmacophore moiety (Pam2 (S-[2,3-bis(palmitoyloxy)-(R)-propyl])) found in MALP-2. All seven of the compounds elicited an agonist response comparable to Pam_2CSK_4 in the screening assay using the 1 ug/mL concentration.

A second set of compound analogs (**8**-**10**) that retained the N-terminal modification of compound **3**, acetylated PEGO, with different C-terminal variations were screened for TLR2 agonist activity (Table 1). All three of the compounds exhibited significant luminescence intensity relative to the no-ligand control, comparable to the Pam_3CSK_4 positive control and significantly more potent than SAA at both 1 μg/mL and 10 μg/mL (n = 4, p<0.001) (Figure 1B). The fold of enhancement for **8**, **9**, and **10** vs. SAA at 1 μg/mL was 11, 13 and 14, respectively. The fold of enhancement for **8**, **9**, and **10** at 1 μg/mL vs SAA at 10 μg/mL was 4.2, 4.8 and 5.2, respectively.

The agonist potency of compounds **3**, **8**-**13**, Pam_2CSK_4 and Pam_3CSK_4 were characterized over a range of concentrations (0.001 ng/mL to 10 μg/mL) to determine EC_{50} values. The resulting normalized dose-response curves generated by measuring the TLR2 agonistic activity for each compound and EC_{50} values are reported in Table 2 (n = 6 assays for test compounds and n=3 assays for control compounds, R^2 values > 0.94) (Supporting Information Figure 2). Test compounds (**3**, **8**-**10**) are potent TLR2 agonists with low nanomolar EC_{50} values ranging from 20 to 78 nM. Compound **10** had the lowest EC_{50} value (20 nM) (Figure 1C), which is comparable to the EC_{50} values for Pam_2CSK_4 (3.7 nM) and Pam_3CSK_4 (23 nM) positive controls (Supporting Information Figure 2F and 2G). Compounds **11**, **12**, and **13** based on the structure of **10** with N-terminal attachments were determined to retain nanomolar TLR2 agonist activity 204, 39 and 34 nM respectively (Table 2, Figure 1D, Supporting Information Figure 2D and 2E).

In Cyto Binding Assays

Lanthanide-based time-resolved fluorescence (TRF) saturation binding and competition binding assays were performed using TLR2 expressing cell lines. Saturation binding assays determined the K_d for the Eu-DTPA chelate labeled compound **11** was 34, 74 and 78 nM and B_{max} was 114,271, 269,878 and 951,170 AFU for the HEK-293/hTLR2, SU.86.86, and Capan-I cells respectively (n > 3 assays per cell line, R^2 values > 0.96) (Table 3, Figure 2A and Supporting Information Figure 3). Competitive binding assays using compound **11** as the competing ligand determined that the K_i for compounds **10** and **13** is 25 and 11 nM in the HEK-293/hTLR2 cell line respectively; and 91 and 67 nM in the SU.86.86 cell line (n > 4 assays, R^2 > 0.78) (Table 4, Figure 2B and C and Supporting Information Figure 4A and C). Compound **12** exhibited the highest binding affinity in the SU.86.86 cell line with a K_i of 25 nM (n = 4 assays, R^2 = 0.90) (Supporting Information Figure 4B).

In Vivo Immune Response

Compound **10** was evaluated *in vivo* as an immune adjuvant using TriVax. This optimized peptide vaccine, comprised of synthetic peptide representing CD8+ T cell epitopes (Trp1$_{455/9M}$), TLR agonists that function as potent immunologic adjuvants (compound **10**, Pam$_2$CSK$_4$, or Pam$_3$CSK$_4$) and co-stimulatory anti-CD40 monoclonal antibody (Clone; FGk-45.5) to generate large numbers of antigen-specific CD8+ T cells capable of recognizing and killing tumor cells.[1112] For comparison, the well-characterized commercially available synthetic TLR2 agonists, Pam$_2$CSK$_4$ and Pam$_3$CSK$_4$, were also evaluated for their ability to function as immulogic adjuvants this peptide vaccine. The activity of each compound as an immune adjuvant was evaluated *in vivo* by measuring the Trp1$_{455/9M}$-specific CD8+ T cell responses in the blood on days 7, 21 and 34 post-immunization by flow cytometry analysis (n = 3) (Figure 3A). Trp1$_{455/9M}$, a TLR agonist, was tested using the TLR2 functional bioassay and is not a TLR2 agonist (data not shown). The maximum amount of fluorescently stained tetramer positive CD8+ T cells for **10**, Pam$_2$CSK$_4$ and Pam$_3$CSK$_4$ observed on day 7 was 49.6%, 56.6% and 51.7% respectively. The 100% response rate of the tetramer positive CD8+ T cells using **10** as the immune adjuvant observed on day 7 decreased to an average of 25.7% on day 21 and 12.7% on day 34 which were comparable responses to using either Pam$_2$CSK$_4$ or Pam$_3$CSK$_4$ (Figure 3B). Therefore these results indicate that compound **10** exhibited activity similar to the other known TLR2 agonists, Pam$_2$CSK$_4$ and Pam$_3$CSK$_4$, for the generation and persistence of antigen-specific CD8+ T cells. No signs or symptoms of stress or toxicity were observed in the mice over the course of the experiment.

In Vivo Tumor Selectivity

Compound **13**, conjugated to a near-infrared fluorescent dye, IRDye800CW, was used to determine *in vivo* TLR2 binding and selectivity for TLR2 expressing tumor xenografts (SU. 86.86 cells). At 24 h post-injection, *in vivo* fluorescence imaging detected retention of fluorescence signal in the tumor (Figure 4A). To determine the *in vivo* selectivity of **13** for TLR2, a blocking study was performed. A significant reduction in the tumor fluorescence was observed 24 h post-injection in the blocked group that received a 20-fold excess of Pam$_2$CSK$_4$ co-injected with **13** compared to the unblocked group receiving only **13** (p < 0.001, n = 8) (Figure 4A and B). The mean unblocked tumor fluorescence was 1.94-fold higher than the blocked. *Ex vivo* imaging confirmed that the fluorescence was associated with the tumors and that the blocked tumors had decreased fluorescence compared to the unblocked tumors (Figure 4C and D). IHC staining (Figure 4E and F) confirmed TLR2 expression in the tumors.

DISCUSSION AND CONCLUSIONS

We first investigated the SAR of a set of novel, fully synthetic compounds (**1**-**7**) through manipulation at the N-terminal portion of MALP-2 derived LPs to enhance TLR2 specificity, potency and binding affinity. Our TLR2 functional bioassay determined that these seven compounds had human TLR2 agonist activities comparable to the reference compounds, Pam_2CSK_4 and Pam_3CSK_4. This result demonstrated that the addition of palmitoyl, fluorescein, Ac-PEGO, Ac-Aha , adapaleneyl, Ac-Aun and tretinoyl groups on MALP-2 derived LPs did not inhibit agonist activity.

The novel TLR2 agonist analogs (**8**-**10**) of compound **3** were designed to alter the chemical properties of the parent compound in order to identify SAR that contributes to increased specificity and binding affinity. This set of compounds was derived from different origins with the goal of altering the compound properties to be more hydrophilic and soluble. Attachment of a modified CD14 peptide (**8**) or the linker Gly-DSer-PEGONH$_2$ (**10**) were both found to enhance the potency, with EC_{50} values of 25 and 20 nM respectively, compared to **3** (EC_{50} = 56 nM). The simplest and smallest compound (**10**), without inclusion of peptide, had the highest potency. Hence, the palmitoyl groups are the minimal binding/ active component and the PEGO groups or peptides serve solely to increase solubility. The IRDye800CW fluorescent dye attachment (**13**) also exhibited a similar potency (EC_{50} = 34 nM) to its unlabeled version (**10**) indicating that dye attachment did not significantly decrease TLR2 agonist activity. However the addition of Eu-DTPA chelate (**11**) resulted in a 10-fold decrease in potency (EC_{50} = 204 nM). Compound **9** was synthesized by attachment of a *S. aureus* peptide to **3**, decreasing the potency (EC_{50} = 78 nM). The *S. aureus* peptide was predicted to be more acidic or at least neutral compared to SAA, with potential to improve potency. Indeed, **9** was observed to have 13-fold higher potency compared to SAA.

The SAR of novel TLR agonist compounds is typically explored using various reporter gene or functional cell-based assays.[22] In order to discover high affinity binding ligands for development of TLR2 targeted agents, we developed a lanthanide-based TRF competition binding assay. We have previously been successful in the characterization of ligand binding affinities for other receptors using this method.[23] For this purpose, compound **11** was synthesized by attachment of Eu-DTPA chelate to the potent TLR2 agonist compound **10**. Saturation binding confirmed the high TLR2 binding affinity of **11** (< 100 nM K_d), which was then used as the competing ligand in competition binding assays that confirmed the high affinities of compounds **10**, **12** and **13** (< 100 nM K_i), which also correlated with high agonist potencies. Although **11** exhibited a 10-fold reduction in potency compared to **10**, high binding affinity was achieved.

In performing the saturation binding assays with **11**, we observed a difference in the K_d values obtained in the HEK-293/hTLR2 cell line, which were genetically engineered to highly over express TLR2, compared to the 2 human pancreatic cells lines, SU.86.86 and Capan-1, that express lower endogenous levels of TLR2.[16] Similar results were also seen in the competition binding assays for both **10** and **13**, in which a reduction in binding affinity for SU.86.86 cells was observed compared to the engineered cell line. Since these TRF binding assays are performed using living cells and the ligand incubation step is longer than the time needed for receptor mediated uptake, off rates may be reduced in a receptor dependent manner and differences observed in the K_d and K_i values obtained from the different cell lines is likely due to the varying levels of TLR2 expression. Using TLR agonists as vaccine adjuvants is a promising application that has been explored to prevent and treat cancer. We have previously reported that the use of TLR agonists as immune adjuvants in peptide vaccination together with anti-CD40 monoclonal antibodies can increase the magnitude and duration of T cell responses resulting from various types of

immunizations including peptide vaccines.[10-11] Results herein show that compound **10** induced an *in vivo* immune response comparable to the currently available TLR2 synthetic agonists (Pam$_2$CSK$_4$ & Pam$_3$CSK$_4$) demonstrating that it can function as an immune adjuvant for use in cancer immunotherapy. Others have also reported that TLR2 agonistic LPs, based on the Pam$_2$CS platform, have a potential role as vaccine adjuvants.[24] It is also worth noting that no signs or symptoms of stress or toxicity were observed in the mice over the course of the study. Kimbrell *et al*. reported that LPs are extremely potent TLR2 agonists *in vivo* with no apparent toxicity in animal models.[25]

The potential use of TLR2 agonist ligands in targeted pancreatic cancer imaging and treatment was explored. We demonstrated the tumor specific retention of the fluorescently labeled compound **13**, *in vivo*, using mice bearing TLR2 expressing xenografts (SU.86.86 cells). Since we previously identified TLR2 as a pancreatic cancer cell surface marker expressed in over 70% of pancreatic tumors but not in normal pancreas tissue, compound **13** could potentially be used for intraoperative detection of pancreatic cancer leading to increased negative resection margins and increased pancreatic cancer survival.

EXPERIMENTAL SECTION

Compound Synthesis, Acquisition and Preparation

Compounds were prepared as previously published by solid-phase synthesis on Rink Amide Tentagel resin (0.23 mmol/g) using Fmoc/*t*Bu synthetic strategy and standard DIC-HOBt and HBTU or HCTU activations.[26] The synthesis was performed in fritted syringes using a Domino manual synthesizer obtained from Torviq (Niles, MI). For compound **3**, **8**-**13**, an Fmoc-protected version of PEGO (Novabiochem, San Diego, CA) was used and an Fmoc protected derivative of Cys, Fmoc-Cys(*S*-[2,3-bisacyloxy-(R)-propyl])-OH (Fmoc-Dhc(Pam$_2$)-OH) was synthesized as described in Supporting information.[27] All compounds were fully deprotected and cleaved from the resin by treatment with 91% TFA (3% water, 3% EDT, and 3% TA) or 90% TFA (5% water, 5% TIS). After ether extraction of scavengers, compounds were purified by HLPC and/or size-exclusion chromatography (Sephadex G-25, 0.1 M acetic acid) to > 95% purity. All compounds were analyzed for purity by analytical HPLC and MS by ESI or MALDI-TOF (synthetic details are in Supporting information).

Materials—N$^\alpha$-Fmoc protected amino acids, HBTU, and HOBt were purchased from SynPep (Dublin, CA) or from Novabiochem (San Diego, CA). Rink amide Tentagel S resin was acquired from Rapp Polymere (Tubingen, Germany). HOCt, DIC and DIEA were purchased from IRIS Biotech (Marktredwitz, Germany). The following side chain protecting groups were used for the amino acids: Arg (N^g-Pbf); Asn (N^{am}-Trt); Asp(*O*-*t*Bu); Glu (*O*-*t*Bu); His (N^{im}-Trt); Ser (*t*Bu), DSer (*t*Bu), Lys (Nε-Boc). An Fmoc-protected version of PEGO was purchased from Novabiochem. IRDye800CW maleimide was kindly provided by LI-COR (Lincoln, NE). Adapalene was purchased from AK Scientist (aksci.com). Peptide synthesis solvents, dry solvents, and solvents for HPLC (reagent grade), and trans-Retinoic acid, were acquired from VWR (West Chester, PA) or Sigma-Aldrich (Milwaukee, WI), and were used without further purification unless otherwise noted. Compounds were manually assembled using 5 to 50 mL plastic syringe reactors equipped with a frit, and a Domino manual synthesizer obtained from Torviq (Niles, MI). The C-18 Sep-Pak™ Vac RC cartridges for solid phase extraction were purchased from Waters (Milford, MA).

Peptide Synthesis—Ligands were synthesized on Tentagel Rink amide resin (initial loading: 0.2 mmol/g) using N$^\alpha$-Fmoc protecting groups and a standard DIC/HOCt or HBTU/HOBt activation strategy. The resin was swollen in THF for an hour, washed with

DMF, and the Fmoc protecting group removed with 20% piperidine in DMF (2 min + 20 min). The resin was washed with DMF (3X), DCM (3X), 0.2 M HOBt in DMF (2X), and finally with DMF (2X) and the first amino acid coupled using pre-activated 0.3 M HOCt ester in DMF (3 eq. of N^α-Fmoc amino acid, 3 eq. of HOCt and 6 eq. of DIC). An on-resin test using Bromophenol Blue was used for qualitative and continuous monitoring of reaction progress. To avoid deletion sequences and slower coupling rate in longer sequences, the double coupling was performed at all steps with 3 eq. of amino acid, 3 eq. of HBTU and 6 eq. of DIEA in DMF. Wherever beads still tested Kaiser positive, a third coupling was performed using the symmetric anhydride method (2 eq. of amino acid and 1 eq. of DIC in dichloromethane). Any unreacted NH_2 groups on the resin thereafter were capped using an excess of 50% acetic anhydride in pyridine for 5 min. When the coupling reaction was finished, the resin was washed with DMF, and the same procedure was repeated for the next amino acid until all amino acids were coupled. Fmoc-PEGO, FmocAha, Fmoc-Aun, Tretinoic acid, Adapalene, and Fluorescein were attached to the resin as symmetrical anhydride (6 eq of acid and 3 eq of DIC in DCM-DMF).

Cleavage of Ligand from the Resin—A cleavage cocktail (10 mL per 1 g of resin) of TFA (91%), water (3%), triisopropylsilane (3%), and 1,2-ethylenedithiol (3%) was injected into the resin and stirred for 4 h at room temperature. Alternatively, a cleavage cocktail of 90% trifluoroacetic acid (5% water, and 5% triisopropylsilane) was used. The crude ligand was isolated from the resin by filtration, the filtrate was reduced to low volume by evaporation using a stream of nitrogen, and the ligand was precipitated in ice-cold diethyl ether, washed several times with ether, dried, dissolved in water and lyophilized to give off-white solid powders that were stored at −20°C until purified. The crude compound was purified by size-exclusion chromatography.

Synthesis of Compound 11, Eu-DTPA Labeled Compound—Attachment of DTPA to the N-terminus of was performed using preformed HOBt activation (3 equiv. DTPA anhydride and 6 equiv. HOBt, Scheme 1). DTPA was attached to H-PEGO-Dhc(Pam$_2$)-Gly-DSer-PEGO-resin as follows. Briefly, DTPA anhydride (3 equiv.) and HOBt (3 equiv.) in DMSO were heated until dissolved (60°C) then stirred for 30 min at room temperature. The preformed DTPA-OBt diester was injected into the free-amine HPEGO-Dhc (Pam$_2$)-Gly-DSer-PEGO-resin and stirred overnight. The resin was washed with DMSO, THF, 5% DIEA 5% water in THF (5 min), THF, and DCM. The compound was cleaved from the resin as described above and purified by HPLC. The purified peptide was dissolved in 0.1 M ammonium acetate buffer pH 8.0, 3.0 eq. Eu(III)Cl$_3$ was added and the reaction was stirred at room temperature overnight. The Eu-labeled peptide was separated using Solid-Phase Extraction (SPE) and lyophilized to yield an amorphous white powder. The final compound was characterized by HPLC (TEAA buffer pH 6.0), ESI-MS and/or FT-ICR.

Synthesis of Compounds 12 and 13—Attachment of Trt-Mpr-OH (*S*-trityl-3-mercaptopropionic acid) to the N-terminus H-PEGO-Dhc(Pam$_2$)-Gly-DSer-PEGO-resin was performed using preformed HBTU activation (3 equiv. of Trt-Mpr-OH, 3 equiv. of HBTU and 6 equiv. of DIEA in DMF) (Scheme 1). The resin was washed with DMF and DCM. The compound **12** was cleaved from the resin as described above and purified by HPLC.

The compound **12** H-Mpr-PEGO-Dhc(Pam$_2$)-Gly-DSer-PEGO-NH$_2$ (1 µmol) was dissolved in 1 mL DMF and reacted with 1 equiv. of IRDye800CW maleimide under argon atmosphere. The reaction was monitored by HPLC and additional aliquots (0.1 equiv.) of dye were added until the reaction complete. The compound was purified by HPLC. The conjugate, compound **13** IRDye800CW-Mpr-PEGO-Dhc(Pam$_2$)-Gly-DSer-PEGO-NH$_2$, was purified by HPLC.

Purification and Analysis—Purity of the peptides was ensured using analytical HPLC (Waters Alliance 2695 separation model with a dual wavelength detector Waters 2487) with a reverse-phase column (Waters Symmetry, 3.0· 75 mm, 3.5 µm; flow rate = 0.3 mL/min). HPLC conditions were as follows: HPLC pH 2, linear gradient from 10 to 90 % B over 30 min, where A is 0.1% TFA and B is acetonitrile or THF, HPLC pH 6, linear gradient from 10 to 90 % B over 30 min, where A is 0.1 % TEAA and B is acetonitrile or THF. Size exclusion chromatography was performed on a borosilicate glass column (2.6 × 250 mm, Sigma, St. Louis, MO) filled with medium sized Sephadex G-25 or G-10. The compounds were eluted with an isocratic flow of 1.0 M aqueous acetic acid.

Solid-Phase Extraction (SPE) was employed where simple isolation of final compound was needed from excess salts and buffers for e.g., lanthaligand synthesis. For this purpose, C-18 Sep-Pak™ cartridges (100 mg or 500 mg) were used and pre-conditioned initially with 5 column volumes (5 times the volume of packed column bed) each of acetonitrile, methanol, and water, in that order. After loading the compound, the column was washed several times with water, and then gradually with 5, 10, 20, 30, 50, and 70 % of aqueous acetonitrile to elute the peptide. Structures were characterized by ESI (Finnigan, Thermoquest LCQ ion trap instrument), MALDI-TOF or FT-ICR mass spectrometry. An appropriate mixture of standard peptides was used for internal calibrations.

The test compounds (**1-13**) were dissolved in DMSO at a 1 mg/mL concentration as stock solutions stored at −20°C. For biological experimental use, 10 µg/mL working solutions of the compounds were prepared from stock solutions in sterilized, deionized water and used immediately.

Acquisition of Commercially Available Compounds and Antibodies—
Commercially available synthetic TLR2 agonists were used as references: Pam_2CSK_4 and Pam_3CSK_4 were purchased from InvivoGen (San Diego, CA) and recombinant human apo-SAA1 was purchased from PeproTech (Rocky Hill, NJ).

$Trp1_{455/9M}$(TAPDNLGYM) is an H-2D^b-optimized peptide for MHC class I binding[28] was obtained from A&A Labs (San Diego, CA). Rat anti-mouse CD40 monoclonal antibody was prepared from the FGK45.5 hybridoma culture supernatants.[11] FITC-conjugated anti-MHC class II and PerCP Cy5.5-conjugated CD8a antibodies were both purchased from eBioscience (San Diego, CA). Phycoerythrin-conjugated $Trp1_{455/9M}$ / H-2D^b tetramers were provided by the NIH Tetramer Facility, Emory University (Atlanta GA).

Cell Culture

The parental HEK-293 cells (ATCC CRL-1573·) and Capan-I cells (ATCC HTB-79) were cultured in DMEM/F12 media (Life Technologies Gibco) supplemented with 10% normal calf serum (NCS) (Atlanta Biologicals, Lawrenceville, GA) and 1% penicillin/streptomycin solution (Sigma). The HEK-293/hTLR2 cells (InvivoGen, San Diego, CA) were cultured in DMEM/F12 media supplemented with 10% NCS, 1% penicillin/streptomycin solution, 10 ug/mL blasticidin (InvivoGen). The SU.86.86 cells (ATCC CRL-1837) were grown in RPMI 1640 media (Life Technologies Gibco) supplemented with 10% NCS. All cells were grown at 37°C and 5% CO_2.

The HEK-293/hTLR2 cells were genetically engineered to highly overexpress TLR2 by stable transfection of the parental HEK-293 cells with pUNO-hTLR2 plasmid expressing the human TLR2 gene.[29] The expression of human TLR2 in HEK-293/hTLR2 cells and absence in the parental HEK-293 cells was confirmed by RT-PCR and western blot analysis (Supporting Information Figure 1A and B). The two human pancreatic cells lines used in our studies, SU.86.86 and Capan-I, express endogenous levels of TLR2.[16]

In vitro TLR2 Functional Bioassay

The *in vitro* TLR2 functional bioassay was developed and optimized for use in high-throughput screening of soluble compound libraries to identify both TLR2 agonists and antagonists. The bioassay measures the induction of NF-κB signaling via TLR2 in HEK-293/hTLR2 cells and parental HEK-293 cells as a negative control. Cells were seeded at a density of 40,000 per well using a WellMate Microplate dispenser (Thermo Fisher Scientific/ Matrix) in black 96-well plates with opaque white wells (PerkinElmer, Waltham, MA) and then incubated at 37°C. On day 2, the cells were transiently transfected with pNifty-Luc(InvivoGen, San Diego, CA), an NF-κB inducible reporter plasmid expressing the luciferase reporter gene[29] using an optimized 4:1 ratio by volume of FugeneHD Transfection Reagent (Promega, Madison, WI) to pNifty-Luc plasmid DNA (1 μg/mL). On day 3, the cells were stimulated with either test peptides or controls adjusted to a final concentration of 1 μg/mL using a NanoDrop Spectrophotometer, ND1000 (Thermo Fisher Scientific). Synthetic di- and tri-acylated LP ligands, Pam_2CSK_4 and Pam_3CSK_4 (InvivoGen), were used as positive controls, TNF-α (InvivoGen) was also used as a transfection control that induces NF-κB independently of TLR2. On day 4 after 24 h of peptide stimulation, luciferase induced activity by the induction of NF-κB was measured. Media was aspirated from the wells using an ELx405 SelectCW plate washer (BioTek, Winooski, VT), 150 μg/mL D-luciferin (Gold Biotechnology, St. Louis, MO) was dispensed using the microplate dispenser; the plates were incubated at 37°C for 5 min. The luminescence intensity was measured using the standard luminescence protocol on a Victor X4 Multilabel plate reader equipped with a plate stacker for readout of multiple plates at a time (PerkinElmer, Waltham, MA). For each *in vitro* TLR2 bioassay, at least three different experiments were performed in triplicate (n 3). Data were analyzed with GraphPad Prism software and curves were generated with the appropriate nonlinear fit regression analysis.

In Cyto Europium Time-Resolved Fluorescence Binding Assays

Europium TRF binding assays were performed as previously described with slight modifications using three cell lines that express TLR2: HEK-293/hTLR2, SU.86.86, and Capan-I.[23a, 23d, 30] The Capan-I and SU.86.86 cells were plated in 96-well black plates with white opaque wells(PerkinElmer); while the HEK-293/hTLR2 cells were plated on 96-well poly-D-lysine coated plates (Sigma-Aldrich) to aid in the attachment of these cells to the plate. Cells were grown in the 96-well plates for 2 days reaching approximately 80% confluency. Both types of plates were evaluated for nonspecific binding and background signal.

For saturation binding, increased concentrations of the labeled ligand, compound **11** (Table 3), were used to determine total binding to TLR2. Non-specific binding was determined in the presence of 1 μM Pam_2CSK_4. On the day of the experiment the medium was aspirated. 50 μL of binding buffer was added to the total binding wells and 50 μL of Pam_2CSK_4 was added to the non-specific wells and then allowed to incubate for 30 min at 37°C. Next, 50 μL of the serial dilutions of **10** were added and then allowed to incubate for 1 h at 37°C. Cells were washed three times to remove unbound ligand. Next, 100 μL of DELFIA Enhancement Solution (PerkinElmer) was added to each well. Cells were incubated for 30 min at 37 °C prior to reading. The plates were read on the VICTOR X4 Multilabel plate reader using the standard europium TRF protocol (340 nm excitation, 400 μs delay and 400 μs emission collection at 615 nm). To determine the mean K_d, statistical analysis was performed using GraphPad Prism software.

Competition binding assays were performed to test the TLR2 binding specificity of the test ligands using 2 cell lines: HEK-293/hTLR2 and SU.86.86. Cells were grown in 96-well plates for 2 days reaching approximately 80% confluency. On the day of the experiment, the

cell culture media was aspirated and 50 μL of nonlabeled test ligand was added in a series of decreasing concentrations (1 μM to 0.01 nM) followed by 50 μL of the competing Eu-labeled ligand **10** at a fixed concentration of 90 nM. Cells were incubated with labeled and unlabeled ligands for 1 h at 37°C. Following incubation, cells were washed three times to remove unbound ligand. Next, 100 μL of DELFIA Enhancement Solution (PerkinElmer) was added to each well. Cells were incubated for 30 min at 37 °C prior to reading. The plates were read on PerkinElmer VICTOR X4 Multilabel reader using the standard europium TRF protocol. To determine the mean K_i, statistical analysis was performed using GraphPad Prism software.

Animal Studies

All procedures were in compliance with the Guide for the Care and Use of Laboratory Animal Resources (1996), National Research Council, and approved by the Institutional Animal Care and Use Committee, University of South Florida. Mice are housed in a clean facility with special conditions that include HEPA filtered ventilated cage systems, autoclaved bedding, autoclaved housing, autoclaved water, irradiated food and special cage changing procedures. Mice are handled under aseptic conditions including the wearing of gloves, gowns and shoe coverings.

In Vivo Cellular Immune Response Assays

To assess the efficacy of **10** as an immune adjuvant, we tested it in our previously reported optimized peptide vaccine, TriVax, comprised of synthetic peptides, TLR agonists and anti-CD40 antibodies.[11] 6-8 week old C57BL/6 (B6) mice (Charles River,Wilmington, MA) were immunized *i.v.* with a mixture (in a volume of 200 μL) of 100 μg optimized $Trp1_{455/9M}$ peptide,[28] 50 μg anti-CD40 monoclonal antibody (Clone; FGk-45.5),[11] and 50 μg TLR2 agonist (**10**, Pam_2CSK_4, or Pam_3CSK_4). The $Trp1_{455/9M}$ peptide (TAPDNLGYM) is a heterocyclic analog of the tyrosinase-related protein-1 (Trp1) sequence.[28] $Trp1_{455/9M}$ is presented to CD8+ T cells via the $H-2D^b$ MHC I molecules to elicit an immune response.[28] $Trp1_{455/9M}$ has increased biostability, enhanced CD8+ T cell response with no CD4+ T cell response for an improved immune induction in the TriVax vaccine.[6a] The cellular immune response of $Trp1_{455/9M}$ / $H-2D^b$ tetramer positive CD8+ T cells in the blood was measured on days 7, 21 and 34. Cellular immune responses were analyzed by tetramer staining, in which tetramers, comprised of synthetic tetrameric MHC class I peptide complexes, are used to stain antigen-specific T cells by FACS analysis. [6b, 31] For tetramer staining, peripheral blood was taken from the submandibular vein and treated briefly with ammonium chloride buffer to lyse red blood cells. Blood cells were stained for 40 min on ice with PerCP Cy5.5-conjugated CD8a antibody to determine CD8+ T cell expression, phycoerythrin-conjugated $Trp1_{455/9M}$ / $H-2D^b$ tetramers for identification of MHC I presentation of $Trp1455_{/9M}$ / $H-2D^b$ and FITC-conjugated anti-MHC class II antibody as a control for non-specific binding of the tetramers by MHC II positive cells, e.g. macrophages. Fluorescence was evaluated using a FACSCalibur flow cytometer (BD Biosciences), tetramer positive CD8+ T cells identified by gating and analyses were performed using FlowJo software. Fluorescence was evaluated using a FACSCalibur flow cytometer (BD Biosciences), $Trp1_{455/9M}$ / $H-2D^b$ tetramer positive CD8+ T cells identified by gating and analyses were performed using FlowJo software.

In Vivo TLR2 Selectivity Experiment

Female athymic nude mice 6-8 weeks old (Harlan) bearing human pancreatic tumor xenografts consisting of SU.86.86 cells on the right flank were used for this study. Mouse weights and tumor volumes were determined using caliper measurements and the formula: volume (mm^3) = (length × $width^2$) / 2. Images were acquired when the tumors reached an

average size of 500 mm^3. For the blocked group, a co-injection of 100 nmol/kg of the fluorescently labeled compound **13** plus 2 μmol/kg Pam$_2$CSK$_4$ (a 20-fold excess) was administered via tail vein injection; for the unblocked group, 100 nmol/kg **13** was administered. Fluorescence images were acquired at time 0 and 24 h using the Caliper Xenogen IVIS200 system (PerkinElmer) with the 710-760 nm excitation and 810-875 nm emission filter set. The fluorescence was quantified using Living Image software, in which the quantified signals were corrected for both instrument and mouse background subtractions. The quantified fluorescence was then plotted using GraphPad Prism software and underwent statistical analysis using Student's t-test.

For further confirmation of ligand **13** specificity for TLR2, ex vivo fluorescence imaging and histological analyses were performed on the tumors. For histological analyses the samples were fixed in 10% formalin solution, processed, embedded, sectioned and either H&E stained for the presence of tumor or underwent IHC staining using TLR2 antibody (Abcam #ab24192).

Statistical Analysis

The results are represented as mean ± s.d. and statistically evaluated by Student's *t* test to determine statistical significance.

Supplementary Material

Refer to Web version on PubMed Central for supplementary material.

Acknowledgments

ABBREVIATIONS

The following additional abbreviations are used:

Boc	*tert*-butyloxycarbonyl
BB	bromophenol blue
***t*-Bu**	*tert*-butyl
CH$_3$CN	acetonitrile
DCM	dichloromethane
DI	de-ionized
DIPEA	diisopropylethylamine
Dhc	2,3-dihydroxypropylcysteine or Cys(*S*-[2,3-hydroxy-(R)-propyl] residue
DMF	*N,N*-dimethylformamide
DIC	diisopropylcarbodiimide
DMEM	Dulbecco's Modified Eagle Medium

Eu-DTPA	europium diethylenetriaminepentaacetic acid
Fmoc	9-fluorenylmethoxycarbonyl
FT-ICR	Fourier Transform-Ion Cyclotron Resonance
ESI-MS	Electrospray ionization-mass spectrometry
EDT	1,2-ethanedithiol
Et$_2$O	Diethyl ether
HBSS	Hank's Balanced Saline Solution buffered with 25 mM Hepes
HCTU	*O*-[1H-6-chloro-benzotriazol-1-yl) (dimethylamino) ethylene] uroniumhexafluorophosphate *N*-oxide
HEPES	4-(2-hydroxyethyl)-1-piperazineethanesulfonic acid
HOBt	*N*-hydroxybenzotriazole
HOCt	6-chloro-1-hydroxybenzotriazole
LP	lipopetide
MALDI-TOF	Matrix Assisted Laser Desorption Ionization-Time of Flight
MALP-2	macrophage-activating lipopeptide 2
Mpr	3-mercaptopropionic residue
PAMP	pathogen-associated molecular patterns
Pbf	2,2,4,6,7-pentamethyl-dihydrobenzofuran-5-sulfonyl
PEGO	19-amino-5-oxo-3,10,13,16-tetraoxo-6-azanonadecan-1-oic acid residue
PRR	pattern recognition receptor
SPPS	solid-phase peptide synthesis
RP-HPLC	reverse-phase high performance liquid chromatography
SAA	serum amyloid a
SAR	structure activity relationship
TA	thioanisole
THF	tetrahydrofuran
TIR	toll/interleukin receptor
TIS	triisopropylsilane
TFA	trifluoroacetic acid
TLR2	toll-like receptor 2
TNF-α	tumor necrosis factor α
TRF	time resolved fluorescence
Trt	trityl

REFERENCES

1 (a). Cheng N, He R, Tian J, Ye PP, Ye RD. Cutting edge: TLR2 is a functional receptor for acute-phase serum amyloid A. J Immunol. 2008; 181(1):22–26. [PubMed: 18566366] (b) Kanzler H, Barrat FJ, Hessel EM, Coffman RL. Therapeutic targeting of innate immunity with Toll-like

receptor agonists and antagonists. Nat Med. 2007; 13(5):552–559. [PubMed: 17479101] (c) Zuany-Amorim C, Hastewell J, Walker C. Toll-like receptors as potential therapeutic targets for multiple diseases. Nat Rev Drug Discov. 2002; 1(10):797–807. [PubMed: 12360257]

2 (a). Jarnicki AG, Conroy H, Brereton C, Donnelly G, Toomey D, Walsh K, Sweeney C, Leavy O, Fletcher J, Lavelle EC, Dunne P, Mills KH. Attenuating regulatory T cell induction by TLR agonists through inhibition of p38 MAPK signaling in dendritic cells enhances their efficacy as vaccine adjuvants and cancer immunotherapeutics. J Immunol. 2008; 180(6):3797–3806. [PubMed: 18322186] (b) Marshall NA, Galvin KC, Corcoran AM, Boon L, Higgs R, Mills KH. Immunotherapy with PI3K Inhibitor and Toll-Like Receptor Agonist Induces IFN-gamma +IL-17+ Polyfunctional T Cells That Mediate Rejection of Murine Tumors. Cancer Res. 2012; 72(3):581–591. [PubMed: 22158905] (c) Adams S. Toll-like receptor agonists in cancer therapy. Immunotherapy. 2009; 1(6):949–964. [PubMed: 20563267]

3 (a). Akira S, Takeda K. Toll-like receptor signalling. Nat Rev Immunol. 2004; 4(7):499–511. [PubMed: 15229469] (b) West AP, Koblansky AA, Ghosh S. Recognition and signaling by toll-like receptors. Annu Rev Cell Dev Biol. 2006; 22:409–437. [PubMed: 16822173]

4 (a). Jin MS, Lee JO. Structures of the toll-like receptor family and its ligand complexes. Immunity. 2008; 29(2):182–191. [PubMed: 18701082] (b) Ozinsky A, Underhill DM, Fontenot JD, Hajjar AM, Smith KD, Wilson CB, Schroeder L, Aderem A. The repertoire for pattern recognition of pathogens by the innate immune system is defined by cooperation between toll-like receptors. Proc Natl Acad Sci U S A. 2000; 97(25):13766–13771. [PubMed: 11095740]

5 (a). Janeway CA Jr. Medzhitov R. Innate immune recognition. Annu Rev Immunol. 2002; 20:197–216. [PubMed: 11861602] (b) Akira S, Takeda K, Kaisho T. Toll-like receptors: critical proteins linking innate and acquired immunity. Nat Immunol. 2001; 2(8):675–680. [PubMed: 11477402] (c) Kawai T, Akira S. The role of pattern-recognition receptors in innate immunity: update on Toll-like receptors. Nat Immunol. 11(5):373–384. [PubMed: 20404851]

6 (a). Cho HI, Lee YR, Celis E. Interferon gamma limits the effectiveness of melanoma peptide vaccines. Blood. 2011; 117(1):135–144. [PubMed: 20889921] (b) Serbina N, Pamer EG. Quantitative studies of CD8+ T-cell responses during microbial infection. Curr Opin Immunol. 2003; 15(4):436–442. [PubMed: 12900276] (c) Ingale S, Wolfert MA, Buskas T, Boons GJ. Increasing the antigenicity of synthetic tumor-associated carbohydrate antigens by targeting Toll-like receptors. Chembiochem. 2009; 10(3):455–463. [PubMed: 19145607] (d) Buskas T, Thompson P, Boons GJ. Immunotherapy for cancer: synthetic carbohydrate-based vaccines. ChemComm. 2009; 36:5335–5349.

7. Hennessy EJ, Parker AE, O'Neill LA. Targeting Toll-like receptors: emerging therapeutics? Nat Rev Drug Discov. 2010; 9(4):293–307. [PubMed: 20380038]

8 (a). Simons MP, O'Donnell MA, Griffith TS. Role of neutrophils in BCG immunotherapy for bladder cancer. Urol Oncol. 2008; 26(4):341–345. [PubMed: 18593617] (b) Murata M. Activation of Toll-like receptor 2 by a novel preparation of cell wall skeleton from Mycobacterium bovis BCG Tokyo (SMP-105) sufficiently enhances immune responses against tumors. Cancer Sci. 2008; 99(7):1435–1440. [PubMed: 18452561]

9. Schmidt J, Welsch T, Jager D, Muhlradt PF, Buchler MW, Marten A. Intratumoural injection of the toll-like receptor-2/6 agonist 'macrophage-activating lipopeptide-2' in patients with pancreatic carcinoma: a phase I/II trial. Br J Cancer. 2007; 97(5):598–604. [PubMed: 17667928]

10. Celis E. Toll-like receptor ligands energize peptide vaccines through multiple paths. Cancer Res. 2007; 67(17):7945–7947. [PubMed: 17804699]

11. Cho HI, Celis E. Optimized peptide vaccines eliciting extensive CD8 T-cell responses with therapeutic antitumor effects. Cancer Res. 2009; 69(23):9012–9009. [PubMed: 19903852]

12. American Cancer Society. Cancer Facts & Figures-2012. American Cancer Society; Atlanta: 2012. p. 1-63.

13 (a). Ferrone CR, Brennan MF, Gonen M, Coit DG, Fong Y, Chung S, Tang L, Klimstra D, Allen PJ. Pancreatic adenocarcinoma: the actual 5-year survivors. J Gastrointest Surg. 2008; 12(4):701–706. [PubMed: 18027062] (b) Howard TJ, Krug JE, Yu J, Zyromski NJ, Schmidt CM, Jacobson LE, Madura JA, Wiebke EA, Lillemoe KD. A margin-negative R0 resection accomplished with minimal postoperative complications is the surgeon's contribution to long-

term survival in pancreatic cancer. J Gastrointest Surg. 2006; 10(10):1338–1345. [PubMed: 17175452]

14 (a). Angst E, Kim-Fuchs C, Chittazhathu Kurian Kuruvilla Y, Inderbitzin D, Montani M, Candinas D, Gloor B. How to counter the problem of r1 resection in duodenopancreatectomy for pancreatic cancer? J Gastrointest Surg. 2012; 16(3):673. [PubMed: 22231631] (b) Esposito I, Kleeff J, Bergmann F, Reiser C, Herpel E, Friess H, Schirmacher P, Buchler MW. Most pancreatic cancer resections are R1 resections. Ann Surg Oncol. 2008; 15(6):1651–1660. [PubMed: 18351300] (c) Campbell F, Smith RA, Whelan P, Sutton R, Raraty M, Neoptolemos JP, Ghaneh P. Classification of R1 resections for pancreatic cancer: the prognostic relevance of tumour involvement within 1 mm of a resection margin. Histopathology. 2009; 55(3):277–283. [PubMed: 19723142]

15 (a). van Dam GM, Themelis G, Crane LM, Harlaar NJ, Pleijhuis RG, Kelder W, Sarantopoulos A, de Jong JS, Arts HJ, van der Zee AG, Bart J, Low PS, Ntziachristos V. Intraoperative tumor-specific fluorescence imaging in ovarian cancer by folate receptor-alpha targeting: first in-human results. Nat Med. 2011; 17(10):1315–1319. [PubMed: 21926976] (b) Sevick-Muraca EM, Sharma R, Rasmussen JC, Marshall MV, Wendt JA, Pham HQ, Bonefas E, Houston JP, Sampath L, Adams KE, Blanchard DK, Fisher RE, Chiang SB, Elledge R, Mawad ME. Imaging of lymph flow in breast cancer patients after microdose administration of a near-infrared fluorophore: feasibility study. Radiology. 2008; 246(3):734–741. [PubMed: 18223125] (c) Tagaya N, Yamazaki R, Nakagawa A, Abe A, Hamada K, Kubota K, Oyama T. Intraoperative identification of sentinel lymph nodes by near-infrared fluorescence imaging in patients with breast cancer. Am J Surg. 2008; 195(6):850–853. [PubMed: 18353274] (d) Stummer W, Pichlmeier U, Meinel T, Wiestler OD, Zanella F, Reulen HJ. Fluorescence-guided surgery with 5-aminolevulinic acid for resection of malignant glioma: a randomised controlled multicentre phase III trial. Lancet Oncol. 2006; 7(5):392–401. [PubMed: 16648043] (e) Hadjipanayis CG, Jiang H, Roberts DW, Yang L. Current and future clinical applications for optical imaging of cancer: from intraoperative surgical guidance to cancer screening. Semin Oncol. 2011; 38(1):109–118. [PubMed: 21362519] (f) Keereweer S, Hutteman M, Kerrebijn JD, van de Velde CJ, Vahrmeijer AL, Lowik CW. Translational Optical Imaging in Diagnosis and Treatment of Cancer. Curr Pharm Biotechnol. 2012; 13(4):498–503. [PubMed: 22214505] (g) Ntziachristos V, Yoo JS, van Dam GM. Current concepts and future perspectives on surgical optical imaging in cancer. J Biomed Opt. 2010; 15(6):066024. [PubMed: 21198198] (h) Nguyen QT, Olson ES, Aguilera TA, Jiang T, Scadeng M, Ellies LG, Tsien RY. Surgery with molecular fluorescence imaging using activatable cell-penetrating peptides decreases residual cancer and improves survival. Proc Natl Acad Sci U S A. 2010; 107(9):4317–4322. [PubMed: 20160097]

16. Morse DL, Balagurunathan Y, Hostetter G, Trissal M, Tafreshi NK, Burke N, Lloyd M, Enkemann S, Coppola D, Hruby VJ, Gillies RJ, Han H. Identification of novel pancreatic adenocarcinoma cell-surface targets by gene expression profiling and tissue microarray. Biochem Pharmacol. 2012; 80(5):748–754. [PubMed: 20510208]

17 (a). Muhlradt PF, Kiess M, Meyer H, Sussmuth R, Jung G. Isolation, structure elucidation, and synthesis of a macrophage stimulatory lipopeptide from Mycoplasma fermentans acting at picomolar concentration. J Exp Med. 1997; 185(11):1951–1958. [PubMed: 9166424] (b) Muhlradt PF, Kiess M, Meyer H, Sussmuth R, Jung G. Structure and specific activity of macrophage-stimulating lipopeptides from Mycoplasma hyorhinis. Infect Immun. 1998; 66(10): 4804–4810. [PubMed: 9746582] (c) Takeuchi O, Kawai T, Muhlradt PF, Morr M, Radolf JD, Zychlinsky A, Takeda K, Akira S. Discrimination of bacterial lipoproteins by Toll-like receptor 6. Int Immunol. 2001; 13(7):933–940. [PubMed: 11431423]

18 (a). Alexopoulou L, Thomas V, Schnare M, Lobet Y, Anguita J, Schoen RT, Medzhitov R, Fikrig E, Flavell RA. Hyporesponsiveness to vaccination with Borrelia burgdorferi OspA in humans and in TLR1- and TLR2-deficient mice. Nat Med. 2002; 8(8):878–884. [PubMed: 12091878] (b) Morr M, Takeuchi O, Akira S, Simon MM, Muhlradt PF. Differential recognition of structural details of bacterial lipopeptides by toll-like receptors. Eur J Immunol. 2002; 32(12):3337–3347. [PubMed: 12432564] (c) Takeuchi O, Sato S, Horiuchi T, Hoshino K, Takeda K, Dong Z, Modlin RL, Akira S. Cutting edge: role of Toll-like receptor 1 in mediating immune response to microbial lipoproteins. J Immunol. 2002; 169(1):10–14. [PubMed: 12077222] (d) Jin MS, Kim SE, Heo JY, Lee ME, Kim HM, Paik SG, Lee H, Lee JO. Crystal structure of the TLR1-TLR2

heterodimer induced by binding of a tri-acylated lipopeptide. Cell. 2007; 130(6):1071–1082. [PubMed: 17889651] (e) Manavalan B, Basith S, Choi S. Similar Structures but Different Roles - An Updated Perspective on TLR Structures. Front Physiol. 2011; 2:41. [PubMed: 21845181] (f) Kang JY, Nan X, Jin MS, Youn SJ, Ryu YH, Mah S, Han SH, Lee H, Paik SG, Lee JO. Recognition of lipopeptide patterns by Toll-like receptor 2-Toll-like receptor 6 heterodimer. Immunity. 2009; 31(6):873–884. [PubMed: 19931471] (g) Buwitt-Beckmann U, Heine H, Wiesmuller KH, Jung G, Brock R, Ulmer AJ. Lipopeptide structure determines TLR2 dependent cell activation level. FEBS J. 2005; 272(24):6354–6364. [PubMed: 16336272] (h) Yamamoto M, Takeda K. Current views of toll-like receptor signaling pathways. Gastroenterol Res Pract. 2010:240365. [PubMed: 21197425]

19. Uhlar CM, Whitehead AS. Serum amyloid A, the major vertebrate acute-phase reactant. Eur J Biochem. 1999; 265(2):501–523. [PubMed: 10504381]

20. Manukyan M, Triantafilou K, Triantafilou M, Mackie A, Nilsen N, Espevik T, Wiesmuller KH, Ulmer AJ, Heine H. Binding of lipopeptide to CD14 induces physical proximity of CD14, TLR2 and TLR1. Eur J Immunol. 2005; 35(3):911–921. [PubMed: 15714590]

21. Fujimoto Y, Hashimoto M, Furuyashiki M, Katsumoto M, Seya T, Suda Y, Fukase K. Lipopeptides from Staphylococcus aureus as Tlr2 Ligands: prediction with mrna expression, chemical synthesis, and immunostimulatory activities. Chembiochem. 2009; 10(14):2311–2315. [PubMed: 19681087]

22. Czarniecki M. Small molecule modulators of toll-like receptors. J Med Chem. 2008; 51(21):6621–6626. [PubMed: 18828583]

23 (a). Handl HL, Vagner J, Yamamura HI, Hruby VJ, Gillies RJ. Development of a lanthanide-based assay for detection of receptor-ligand interactions at the delta-opioid receptor. Anal Biochem. 2005; 343(2):299–307. [PubMed: 16004955] (b) Xu L, Vagner J, Josan J, Lynch RM, Morse DL, Baggett B, Han H, Mash EA, Hruby VJ, Gillies RJ. Enhanced targeting with heterobivalent ligands. Mol Cancer Ther. 2009; 8(8):2356–2365. [PubMed: 19671749] (c) Barkey NM, Tafreshi NK, Josan JS, De Silva CR, Sill KN, Hruby VJ, Gillies RJ, Morse DL, Vagner J. Development of melanoma-targeted polymer micelles by conjugation of a melanocortin 1 receptor (MC1R) specific ligand. J Med Chem. 2011; 54(23):8078–8084. [PubMed: 22011200] (d) Josan JS, Morse DL, Xu L, Trissal M, Baggett B, Davis P, Vagner J, Gillies RJ, Hruby VJ. Solid-phase synthetic strategy and bioevaluation of a labeled delta-opioid receptor ligand Dmt-Tic-Lys for in vivo imaging. Org Lett. 2009; 11(12):2479–2482. [PubMed: 19445485]

24 (a). Agnihotri G, Crall BM, Lewis TC, Day TP, Balakrishna R, Warshakoon HJ, Malladi SS, David SA. Structure-activity relationships in toll-like receptor 2-agonists leading to simplified monoacyl lipopeptides. J Med Chem. 2011; 54(23):8148–8160. [PubMed: 22007676] (b) Salunke DB, Shukla NM, Yoo E, Crall BM, Balakrishna R, Malladi SS, David SA. Structure-Activity Relationships in Human Toll-like Receptor 2-Specific Monoacyl Lipopeptides. J Med Chem. 2012; 55(7):3353–3363. [PubMed: 22385476]

25. Kimbrell MR, Warshakoon H, Cromer JR, Malladi S, Hood JD, Balakrishna R, Scholdberg TA, David SA. Comparison of the immunostimulatory and proinflammatory activities of candidate Gram-positive endotoxins, lipoteichoic acid, peptidoglycan, and lipopeptides, in murine and human cells. Immunol Lett. 2008; 118(2):132–141. [PubMed: 18468694]

26 (a). Vagner J, Xu L, Handl HL, Josan JS, Morse DL, Mash EA, Gillies RJ, Hruby VJ. Heterobivalent ligands crosslink multiple cell-surface receptors: the human melanocortin-4 and delta-opioid receptors. Angew Chem Int Ed Engl. 2008; 47(9):1685–1688. [PubMed: 18205159] (b) Krchnak V, Vagner J, Lebl M. Noninvasive continuous monitoring of solid-phase peptide synthesis by acid-base indicator. Int J Pept Protein Res. 1988; 32(5):415–416. [PubMed: 3209356] (c) Krchnak V, Vagner J. Color-monitored solid-phase multiple peptide synthesis under low-pressure continuous-flow conditions. Pept Res. 1990; 3(4):182–193. [PubMed: 2134062]

27 (a). Metzger JW, Wiesmuller KH, Jung G. Synthesis of N alpha-Fmoc protected derivatives of S-(2,3-dihydroxypropyl)-cysteine and their application in peptide synthesis. Int J Pept Protein Res. 1991; 38(6):545–554. [PubMed: 1819589] (b) Reichel F, Roelofsen AM, Geurts HPM, Hämäläinen TI, Feiters MC, Boons G-J. Stereochemical Dependence of the Self-Assembly of the Immunoadjuvants Pam3Cys and Pam3Cys-Ser. J ACS. 1999; 121(35):7989–7997.

28. Guevara-Patino JA, Engelhorn ME, Turk MJ, Liu C, Duan F, Rizzuto G, Cohen AD, Merghoub T, Wolchok JD, Houghton AN. Optimization of a self antigen for presentation of multiple epitopes in cancer immunity. J Clin Invest. 2006; 116(5):1382–1390. [PubMed: 16614758]

29. Schindler U, Baichwal VR. Three NF-kappa B binding sites in the human E-selectin gene required for maximal tumor necrosis factor alpha-induced expression. Mol Cell Biol. 1994; 14(9):5820–5831. [PubMed: 7520526]

30. Handl HL, Vagner J, Yamamura HI, Hruby VJ, Gillies RJ. Lanthanide-based time-resolved fluorescence of in cyto ligand-receptor interactions. Anal Biochem. 2004; 330(2):242–250. [PubMed: 15203329]

31. Appay V, Rowland-Jones SL. The assessment of antigen-specific CD8+ T cells through the combination of MHC class I tetramer and intracellular staining. J Immunol Methods. 2002; 268(1):9–19. [PubMed: 12213338]
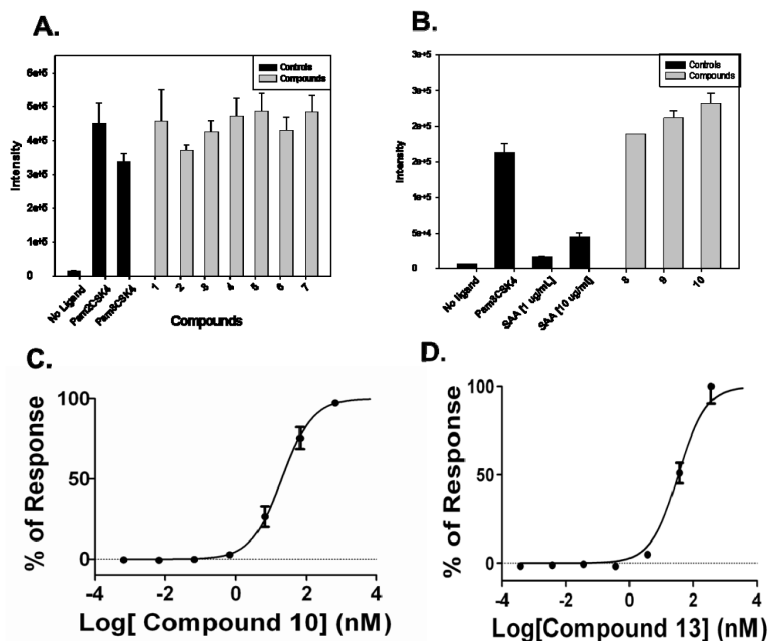
Figure 1.
Screening of A) **X**-Cys(*S*-[2,3-bis(palmitoyl)oxy-(R)-propyl])-MALP-2 derived peptide library (compounds **1**-**7**) and B) compound analogs (**8**-**10**) with an Ac-PEGO-Cys(*S*-[2,3-bis(palmitoyl)oxy-(R)-propyl])-**Y** and SAA for TLR2 agonist activity determined using the functional bioassay. All compounds exhibit high luminescence intensities similar to the TLR2 agonist controls, Pam_2CSK_4 and Pam_3CSK_4, using the HEK-293/hTLR2 cells (n = 3 assays with quadruplicate wells, p value<0.0003). Dose-response curves generated by measuring the TLR2 agonistic activity for C) compound **10** and D) compound **13**. Performed by serially adding (0.001 ng/mL to 10 μg/mL) compound to HEK-293/hTLR2 expressing cells (n > 3 assays with quadruplicate wells, R^2 > 0.98).
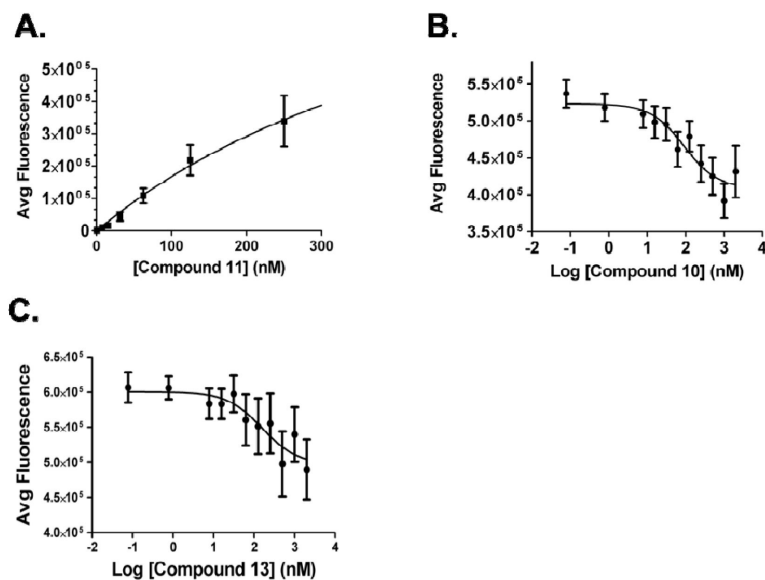
Figure 2.
Mean binding analysis curves generated by *in cyto* TRF binding assays. A) Saturation binding curve shows the specific binding (total – nonspecific) curve of Eu-DTPA-labeled compound **11** to TLR2 using HEK-293/hTLR2 cells with a K_d of 34 nM and B_{max} of 114,271 AFU (n = 3 assays, R^2 values > 0.97). Competition binding analysis, in which increasing concentrations of test compound were added in the presence of 90 nM **11** using HEK-293/hTLR2 cells. B) Compound **10** has a K_i of 25 nM (n = 5 assays, R^2 = 0.90). C) Compound **13** has a K_i of 11 nM (n = 4 assays, R^2 = 0.87).
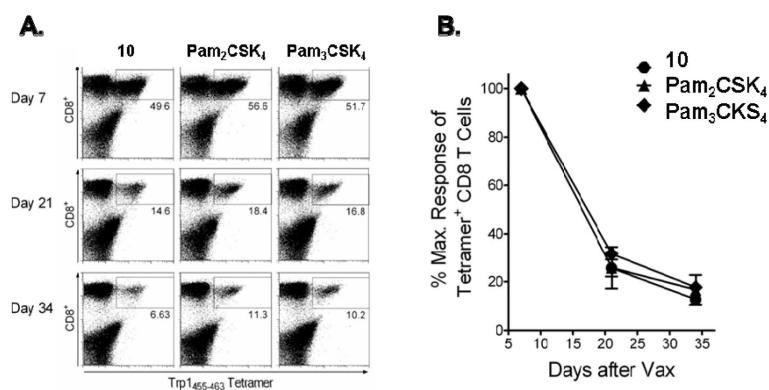
Figure 3.
Evaluation of TLR2 agonists as Immune Adjuvants. B6 mice were immunized *i.v.* with a mixture of $Trp1_{455/9M}$ peptide, anti-CD40 monoclonal antibody plus one of the following TLR2 agonists: **10**, Pam_2CSK_4, or Pam_3CSK_4. A) Antigen-specific CD8+ T cells in peripheral blood were measured on days 7, 21 and 34 by flow cytometry analysis of $Trp1_{455/9M}$/H-2Db tetramer staining. Numbers in each rectangular gate represent the % positive cells of all CD8+ T cells. B) Mean maximum response of antigen-specific CD8+ T cells in peripheral blood for up to 34 days post-immunization (n = 3). Results represent the mean and SD (error bars) of three mice per experimental group.
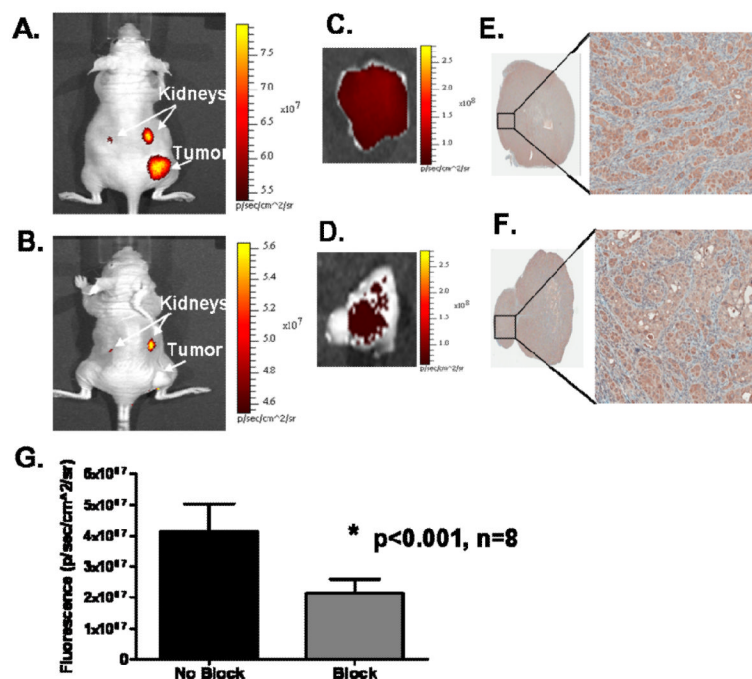
Figure 4.
Comparison of representative fluorescence images of nude mice bearing TLR2 expressing tumor xenografts (SU.86.86 cells) acquired at 24 h, where the A) unblocked mice were administered 100 nmol/kg **13** and B) blocked mice were administered a co-injection of 100 nmol/kg **13** plus 2 μmol/kg Pam_2CSK_4 (20-fold excess). *Ex vivo* tumor selectivity was observed in the *ex vivo* fluorescence images of the unblocked and blocked tumors, C) and D), and the corresponding IHC staining for TLR2, E) and F), respectively. G) Shows the graphed results in which a significant reduction in the *in vivo* fluorescence signal was measured in the blocked tumors compared to the tumors that were not blocked (n = 8, p < 0.001), the mean increase in signal (unblocked tumor/ blocked tumor) of **13** in the tumor was 1.94 fold.
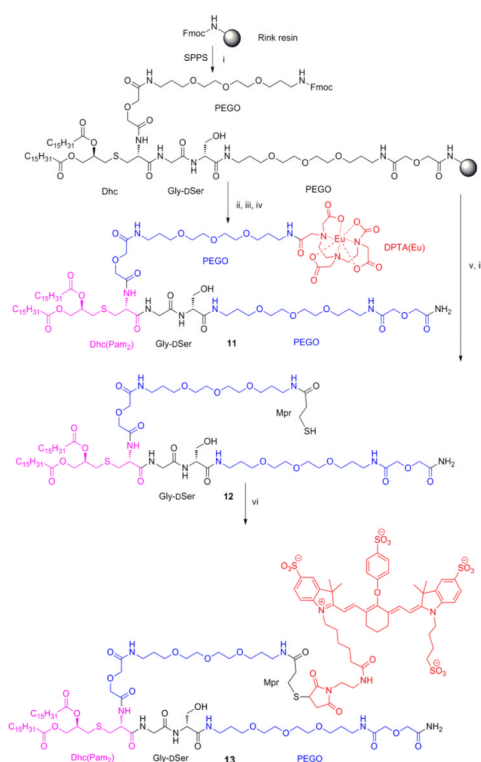
Scheme 1. Synthetic Route for Eu-DTPA Compound 11, Mpr Compound 12 and IRDye800CW Compound 13

[i]Fmoc/tBu synthesis continued as follows: a) Piperidine/DMF (1:4) for Fmoc deprotection; b) Fmoc-aa-OH (3eq), HOBt (3eq), DIEA (6eq), and HBTU (3eq) in DMF for amino acid couplings; [ii] DTPA was attached after Fmoc deprotection as follows: a) DTPA anhydride (3 eq) and HOBt (3 eq) were dissolved in dry DMSO (0.5M), heated to 60°C for 3 min then stirred at room temperature for 30 min, b) preformed DTPA-OBt diester mixture reacts with the resin overnight; [iii] TFA-scavenger cocktail (90% trifluoroacetic acid, 5% water, 5% triisopropylsilane) for 2 h; [iv] Eu(III)Cl$_3$ (3.0 eq.) in 0.1M ammonium acetate buffer pH 8.0 overnight; [v] a) Piperidine/DMF (1:4) for Fmoc deprotection; b) Trt-3-mercaptopropionic acid (3eq), DIEA (6eq), and HBTU (3eq) in DMF; [vi] IRDye800CW maleimide (1 eq) in DMF.

Table 1

Synthesized Compounds.

#	Compounds (X, Y or Z Modifications)	MW calc/found[a]
X-Cys(*S*-[2,3-bis(palmitoyl)oxy-(R)-propyl])-Gly-Asn-Asn-Asp-Glu-Ser-Asn-Ile-Ser-Phe-Lys-Glu-Lys-NH₂		
1	Palmitoyl-	2371.4/ 1186.23(M+2)⁺
2	Fluorescein-	2491.3/ 2492.36
3	Ac-PEGO[b]-	2493.4/ 2494.43
4	Ac-Aha[c]-	2288.3/ 2288.0
5	Adapalenoyl-	2526.4/ 2528.40
6	Ac-Aun[d]-	2358.4/ 2359.41
7	Tretinoyl-	2414.4/ 2415.28
Ac-PEGO-Cys(*S*-[2,3-bis(palmitoyl)oxy-(R)-propyl])-**Y**		
8[e]	-Ser-Arg-Phe-Asp-Glu-Asp-Asp-Leu-Glu-NH₂	2137.2/ 1069.90(M+2)²⁺
9	-Gly-Ser-Gln-Asn-Leu-Ala-Ser-Leu-Glu-Glu-NH₂	2059.2/ 1030.3(M+2)²⁺
10	-Gly-DSer-PEGO-NH₂	1492.95/ 1493.5
Z-PEGO-Cys(*S*-[2,3-bis(palmitoyl)oxy-(R)-propyl])-Gly-DSer-PEGO-NH₂		
11	Eu-DTPA[f]-	1975.98/ 1975.4-1977.4
12	Mpr[g]-	1538.95/ 1539.5
13	IRDye800CW-Mpr-	2728.8/ 1330.60(M+2)²⁺

[a]Found = as determined by mass spectrometery.

[b]PEGO denotes 20 atom ethylene glycol oligomer (the full structure is depicted in the Supporting Information).

[c]Aha denotes 6-aminohexanoyl residue.

[d]Aun denotes 11-aminoundecanoyl residue.

[e]All amino-acid residues are D-configuration.

[f]Eu-DTPA denotes Europium chelated in diethylenetriaminepentaacetic acid.

[g]Mpr denotes 3-mercaptopropionyl residue.

Table 2

TLR2 Agonist Activity (EC_{50} Values) Calculated From Dose-Response Curves.

Compd	EC_{50}		R^2
	(nM)	Std. Error	Value
3	56	1.1	0.99
8	25	1.1	0.99
9	78	1.1	0.99
10	20	1.0	0.99
11	204	1.3	0.97
12	39	1.1	0.98
13	34	1.2	0.98
Pam_2CSK_4	3.7	1.4	0.96
Pam_3CSK_4	23	1.5	0.94

Table 3

TLR2 Binding Affinity (K_d) for Compound 11 Determined by Saturation Binding Assays.

TLR2 Expressing Cell line	K_d		B_{max}		R^2 Value
	(nM)	Std. Error	(AFU)	Std. Error	
HEK-293/hTLR2	34	13	114,271	17,001	0.97
SU.86.86	74	16	269,878	28,809	0.99
Capan-I	78	22	951,170	112,968	0.96

Table 4

TLR2 Binding Affinity (K_i) Determined by Competition Binding Assays.

Compd	TLR2 Expressing Cell line	K_i		R^2 Value
		(nM)	Std. Error	
10	HEK-293/hTLR2	25	1.8	0.89
10	SU.86.86	91	1.4	0.95
12	SU.86.86	25	1.7	0.90
13	HEK-293/hTLR2	11	1.8	0.87
13	SU.86.86	67	2.3	0.78